Phase transitions and octahedral rotations in epitaxial $Ag(Ta_xNb_{1-x})O_3$ thin films under tensile strain

R. L. Johnson-Wilke, R. H. T. Wilke, C. B. Yeager, D. S. Tinberg, I. M. Reaney, I. Levin, D. D. Fong, and S. Trolier-McKinstry

Citation: Journal of Applied Physics **117**, 085309 (2015); doi: 10.1063/1.4913283
View online: http://dx.doi.org/10.1063/1.4913283
View Table of Contents: http://aip.scitation.org/toc/jap/117/8
Published by the American Institute of Physics

Phase transitions and octahedral rotations in epitaxial $Ag(Ta_xNb_{1-x})O_3$ thin films under tensile strain

R. L. Johnson-Wilke,[1] R. H. T. Wilke,[1] C. B. Yeager,[1] D. S. Tinberg,[1] I. M. Reaney,[2] I. Levin,[3] D. D. Fong,[4] and S. Trolier-McKinstry[1]
[1]*Materials Research Institute and Materials Science and Engineering Department, The Pennsylvania State University, University Park, Pennsylvania 16802, USA*
[2]*Department of Engineering Materials, University of Sheffield, Sir Robert Hadfield Building, Mappin Street, Sheffield S1 3JD, United Kingdom*
[3]*Materials Measurement Science Division, National Institute of Standards and Technology, Gaithersburg, Maryland 20899, USA*
[4]*Materials Science Division, Argonne National Laboratory, Argonne, Illinois 60439, USA*

(Received 29 November 2014; accepted 9 February 2015; published online 27 February 2015)

Epitaxial $Ag(Ta_{0.5}Nb_{0.5})O_3$ (ATN) films under tensile strain were deposited on $(Ba_{0.4}Sr_{0.6})TiO_3/LaAlO_3$ $(001)_p$ and $KTaO_3$ (001) substrates. These films exhibited a domain structure with the *c*-axis aligned primarily along the in-plane direction in contrast with the poly-domain nature of bulk ATN ceramics or relaxed films. While the generic phase transition sequence of the tensile films was qualitatively similar to bulk, the tetragonal and orthorhombic phase field regions expanded by ~270 °C in $ATN/(Ba_{0.4}Sr_{0.6})TiO_3/LaAlO_3$. Furthermore, the films were found to be in the M_3 (complex octahedral tilting with disordered Nb/Ta displacements) phase at room temperature with either significantly reduced tilt angles or a suppression of the long range order of the complex tilt as compared to bulk materials. It was observed that the octahedral tilt domains were oriented with the complex tilt axes lying in the plane of the film due to the tensile strain. This work demonstrates that tensile strain can be used to strain-engineer materials with complex tilt systems and thereby modify functional properties. © *2015 AIP Publishing LLC*.
[http://dx.doi.org/10.1063/1.4913283]

INTRODUCTION

New properties in materials crystallizing with perovskite-like structures can be engineered by controlling lattice distortions and rotations of oxygen octahedra. The suppression or enhancement of the octahedra tilting can induce ferroelectric or magnetic states or transform insulators into metals and vice versa.[1,2] For instance, theoretical calculations and experiments have shown that octahedral rotations have the potential to control orbital, magnetic,[3] electronic,[4,5] and dielectric properties of a given material.[2,6] In a thin film of a given composition, oxygen octahedra rotation angles can be manipulated through one of the three mechanisms:[7] epitaxial strain,[8–10] interfacial control at heterojunction interfaces,[11] or rotation engineering in short-period superlattice structures.[12] The present work reports the use of epitaxial strain to control octahedral rotations and ultimately the phase transition temperatures in the complex oxide perovskite material $Ag(Ta_{0.5}Nb_{0.5})O_3$ (ATN).

In perovskite materials, the electrical, magnetic, and structural functionalities result from structural deformations including cation displacements, distortions of the $[BO_6]$ oxygen octahedra, and rotations of the octahedra. Strain engineering has been used extensively to control lattice distortions to induce ferroelectric properties in perovskites such as $SrTiO_3$ and $CaTiO_3$.[13–15] However, the coupling between strain and octahedral rotations is less understood than the coupling between strain and lattice distortions. In general, a perovskite material will undergo cooperative rotations of the oxygen octahedra when the A-site ion (12-fold coordinated by oxygen in the ideal cubic arrangement) is underbonded, as occurs in perovskites with tolerance factors less than 0.985.[16,17] Diffraction (electron, X-ray, or neutron) is typically used to monitor superlattice reflections characteristic of any tilt sequence as well as quantify the rotation angle of octahedral rotations, with "Glazer notation" used to describe the unique combinations of antiphase (−) and in-phase (+) tilting around three orthogonal axes.[16,17]

Through the use of epitaxial strain, May *et al*. have shown that in $LaNiO_3$ thin films subjected to a compressive biaxial strain, the out-of-plane rotation angle was enhanced, while the in-plane rotation angle was suppressed.[8] $LaNiO_3$ films under tensile strain showed the opposite effect (out-of-plane rotation angles was suppressed, while the in-plane rotation angle was enhanced).[8] Density functional theoretical calculations and subsequent experiments showed that the tilt angles in $LaAlO_3$ (LAO) behaved in a similar manner.[9,10,18] Previous work also showed that tilt transition temperatures were strongly affected by in-plane biaxial strain in $SrTiO_3$, $LaAlO_3$, and $Ag(Ta_{0.5}Nb_{0.5})O_3$ films.[18–20] A second mechanism to control octahedral rotations involves interfacial effects. In this case, non-equilibrium rotation patterns can be stabilized across a few unit cells in the vicinity of the interface between the substrate and the film. For instance, Moon *et al*. showed that $La_{2/3}Sr_{1/3}MnO_3$ (LSMO) thin films deposited on a tilted and untilted substrate ($NdGaO_3$ and $(LaAlO_3)_{0.3}(Sr_2AlTaO_6)_{0.7}$, respectively) had substantially different rotation angles near the interface, which ultimately contributed to significant differences in magnetic behavior and electrical conductivity.[21]

Interface effects have also been observed in $LaAlO_3$ films on $SrTiO_3$[18,22] as well as $BiFeO_3$ films on LSMO/$SrTiO_3$.[4] Third, octahedral rotations can be controlled through the use of short period superlattices. For instance, May *et al.* showed that alternating layers of a tilted ($LaNiO_3$) and untilted ($SrMnO_3$) material led to a stabilization of new octahedral rotation patterns.[12] Density functional theory calculations have shown promising avenues for further means of controlling tilt utilizing superlattice structures.[2,7]

The work discussed above describes tilt systems with a single type of octahedral rotation (e.g., in-phase or anti-phase) about a given axis. In contrast, perovskite-like silver tantalate niobate (Ag(Ta, Nb)O_3) exhibits a complex octahedral tilt system at room temperature.[23–27] This tilt system, which in Glazer's notation can be described as $a^-b^-c^-/a^-b^-c^+$, features a sequence of in-phase and anti-phase rotations about one of the axes, resulting in the quadrupled periodicity along this direction; simple anti-phase rotations occur about two other crystal axes (Figures 1(a) and 1(b)). Such a complex tilt system gives rise to a $\sqrt{2}a_p \times \sqrt{2}a_p \times 4a_p$ unit cell at room temperature, where p refers to the pseudocubic cell and $a_p \approx 3.92$Å. Ag(Ta, Nb)O_3 undergoes a complex sequence of phase transitions with temperature. The complex tilting is shared by the so-called M-phases (M3, M2, and M1) that differ by the degree of ordering for the Nb/Ta displacements. On heating, the M3-phase transforms to the orthorhombic (O) phase (with $a^0b^-c^+$ tilt system) at 326 °C and then to a tetragonal (T) phase (with $a^0b^0c^+$ tilt system) at 400 °C before becoming cubic (C) at 552 °C. Previous work examining the tilt transition sequence and rotation patterns has been performed on relaxed and compressively strained Ag(Ta, Nb)O_3 films.[28,29] The current work presents results for Ag($Ta_{0.5}Nb_{0.5}$)O_3 films under tensile strain with an emphasis on phase-transition sequences and domain structures. For ATN films under tensile strain, it was found that the films exhibited the same tilt transition sequence as compared to bulk ATN; however, the high temperature orthorhombic and tetragonal phases were stable over a larger temperature range. In addition, the induced strain enabled orientation control of the domain state at room temperature.

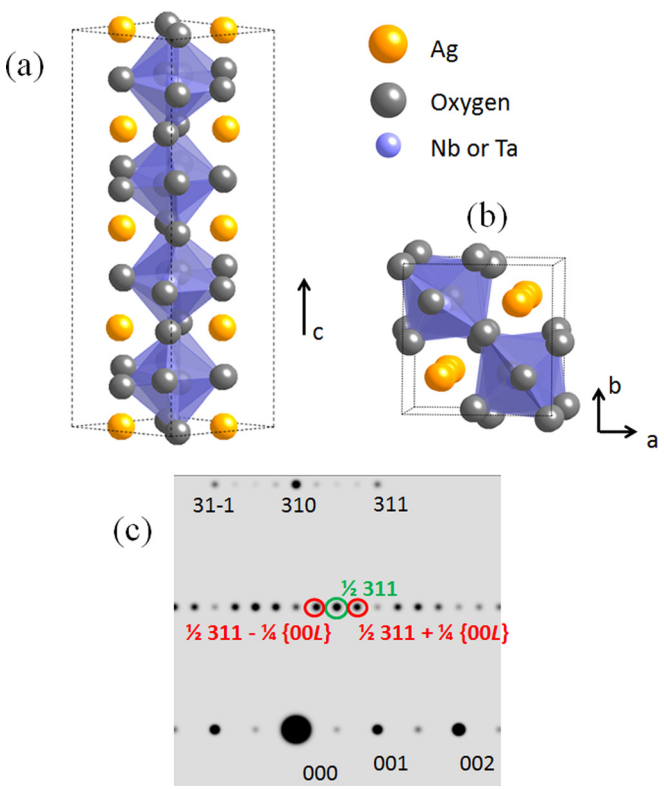

FIG. 1. The unit cell of room temperature Ag($Ta_{0.5}Nb_{0.5}$)O_3 in the M3 phase as (a) viewed along the $\langle 110_o \rangle$ ($\langle 100_p \rangle$) showing quadrupling of the unit cell along the c-direction and (b) viewed down the c-axis showing combined in-phase and anti-phase rotations. (c) Simulated electron diffraction pattern along the $[130]_p = [240]_o$ zone axis for ATN in the M3 phase. The $^1/_2311 \pm {}^1/_4\{00L\}$ spots occur from the quadrupling of the unit cell due to the octahedral tilt system $a^-b^-c^-/a^-b^-c^+$.

EXPERIMENTAL PROCEDURE

To induce a tensile strain in ATN films, the substrate must have a slightly larger lattice parameter and, ideally, should be cubic with no rotation of the oxygen octahedra. Two different substrates were chosen for this purpose: ($Ba_{0.4}Sr_{0.6}$)TiO_3 (BST) $(001)_p$ (where the subscript p indicates pseudocubic notation) and $KTaO_3$ (001). BST has a lattice parameter ~3.94 Å, designed to induce 0.85% tensile strain along the a-axis, negligible strain along the b-axis, and 0.53% strain along the c-axis of coherent ATN films. These strain states were equal, but opposite in magnitude to the strain states in ATN films on $SrTiO_3$ substrates as described by Johnson-Wilke *et al.*[20] Since single crystals of BST are not commercially available, a BST thin film (~150 nm) was grown using pulsed laser deposition on single-crystal $LaAlO_3$ $(001)_p$ to act as a substrate for the Ag(Ta_xNb_{1-x})O_3 layer. LAO was chosen because its lattice parameter differed enough from the BST so that peaks of the two substrate components were readily distinguishable in diffraction patterns. While LAO has a tilt system $a^-a^-a^-$, its superlattice reflections are separated from the analogous tilting-related peaks in ATN. The ATN film thickness on BST/LAO was ~15 nm. The second substrate, $KTaO_3$ (001), is cubic, with a lattice parameter of 3.989 Å. This would induce a 2.0% strain along the a-axis, 1.3% strain along the b-axis, and 1.8% strain along the c-axis in ATN. Due to the larger misfit strain, the ATN film was grown to a thickness of only 7.5 nm to increase the likelihood of coherency.

ATN films were deposited using a chemical solution deposition route. Niobium ethoxide, tantalum ethoxide, and silver nitrate were dissolved in 2-methoxyethanol and pyridine and mixed at 110 °C. The solution was spun on the substrates at 1500 rpm for 30 s followed by two pyrolysis steps at 200 °C and 450 °C. The films were crystallized at 750 °C for 1 min in a rapid thermal annealing furnace. Additional details on the solution preparation are provided elsewhere.[28,30–32]

Structural characterization was performed on the films using both a lab source X-ray diffractometer and the Advanced Photon Source (APS) at Argonne National Lab. At the APS, experiments were performed at 33BM with a photon energy of 21 keV, using a Huber 4-diffractometer with a point detector. Samples were heated to 750 °C and measurements were performed every 25 °C on cooling. Substrate Bragg peaks were recorded at each temperature step in an effort to calibrate the temperature stage using the known thermal

expansion coefficient of $LaAlO_3$. Similarly, the Bragg peaks and superlattice reflections from the ATN films were measured at each temperature. The peaks were background subtracted and fitting was performed using a pseudo-Voigt function to obtain peak positions and integrated intensities.

Cross-sectional samples for transmission electron microscopy (TEM) were prepared using conventional mechanical sectioning, polishing, and dimpling to a thickness of 30 μm. The thinning was completed until perforation in the Gatan Precision Ion Polishing System (PIPS) operated at 4.5 kV and an ion-beam angle of 4.5°. Previously, this procedure was shown to provide artifact-free TEM samples of bulk $AgNbO_3$ and $Ag(Nb,Ta)O_3$. The samples were analyzed using an FEI Titan TEM/STEM operated at 300 kV. Both high-resolution phase-contrast TEM (HRTEM) and high-angle annular dark-field (HAADF) scanning tunneling electron microscope (STEM) images were recorded with the incident electron beam parallel to the [100] zone axis. HAADF images are formed using electrons scattered to high angles and therefore are sensitive to the atomic numbers of the scattering atoms; therefore, this technique is often referred to as Z-contrast imaging.

RESULTS AND DISCUSSION

Figure 2(a) shows a HAADF STEM micrograph of an ATN film on a BST buffer layer. The image shows that the interface contains no amorphous or second phases and the ATN is coherent with the BST. The brighter spots in the ATN's image correspond to Nb/Ta atomic columns, whereas the brighter regions in the images of BST represent the Ba/Sr columns.

Lab source X-ray diffraction was used to determine the phase purity of each sample. No indication of second phases or misorientation was apparent in either the ATN/BST/LAO or ATN/$KTaO_3$ sample. The rocking curve widths of the ATN 002 peaks were 0.11° and 0.058°, for films on BST/LAO and ATN/$KTaO_3$, respectively. The larger width of the ATN film on BST/LAO indicates lower crystal quality than that of ATN on $KTaO_3$.

The room temperature phase can be determined, in part, by the existence or absence of quarter-order reflections flanking the $\frac{1}{2}\{ooo\}$-type reflections (where o = odd index). As described elsewhere, such peaks indicate that the material has the complex tilt system $a^-b^-c^-/a^-b^-c^+$ and is in one of the M phases.[20,23,28] A simulated diffraction pattern showing the existence of such quarter-order reflections for ATN in the M3 phase is shown in Figure 1(c).

Complex tilt in ATN on BST/LAO

Reciprocal space scans along the H, K, and L directions through the $\frac{1}{2}(113)$ reflection for the ATN film on BST are shown in Figure 2(b). No indication of the quarter-order reflection was observed; possible explanations include the film existing in the O phase field at room temperature, a small tilt angle making the superlattice reflections undetectable, or a suppression of the long-range order for the in-phase and anti-phase octahedral rotations.

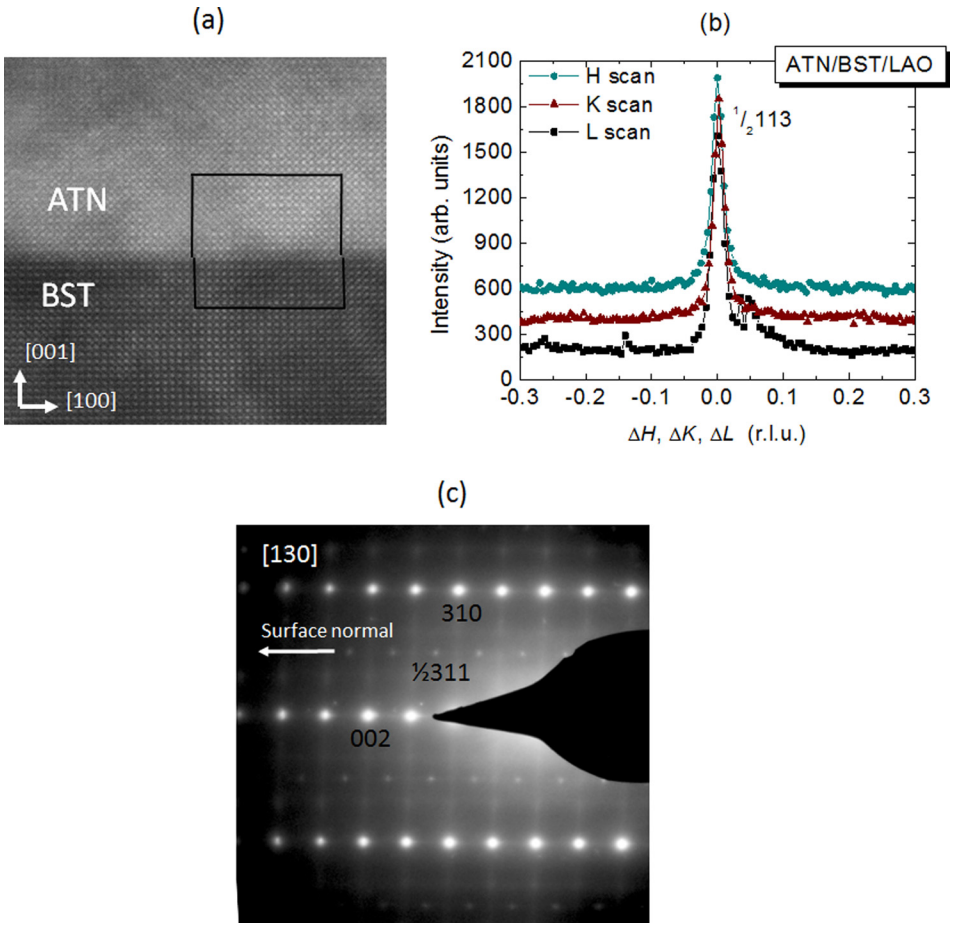

FIG. 2. (a) High resolution TEM of the $Ag(Ta_{0.5}Nb_{0.5})O_3$ film on a $(Ba_{0.4}Sr_{0.6})TiO_3$ layer showing the films are coherent with the buffer layer. (b) Reciprocal space scan around the ATN $\frac{1}{2}(113)$ reflection. No indication of the 1/4 order reflections is present in the XRD data. (c) TEM electron diffraction patterns along the [130] zone axes indicating no evidence of quarter-order reflections about the $\frac{1}{2}\{ooo\}$ spots. Sheets of diffuse intensity suggest that the long range order of the B-site cation ordering is reduced, indicating the films are in the M3 phase.

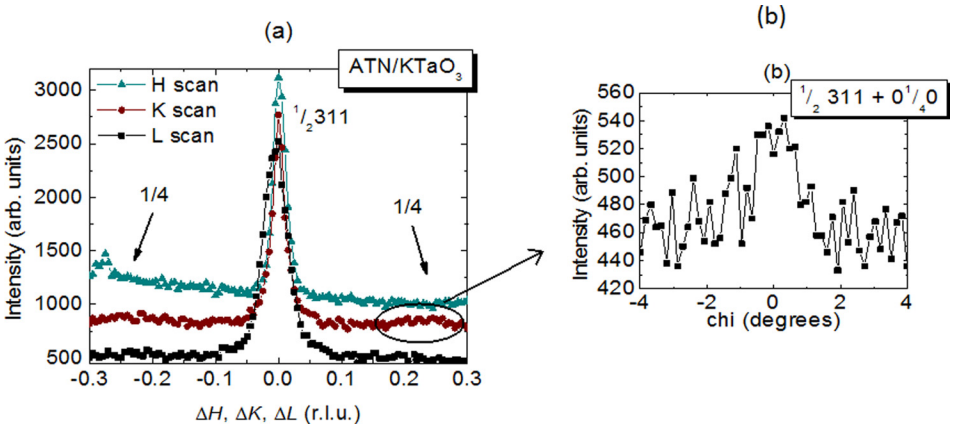

FIG. 3. (a) X-ray diffraction scans of $Ag(Ta_{0.5}Nb_{0.5})O_3$ film on $KTaO_3$. Reciprocal space scans in the H, K, and L directions around the $1/2(311)$ reflection. (b) Plot of chi scans (where chi is defined as rotation about the horizontal axis) near $1/2(311) + 1/4\{0K0\}$ shows a weak peak. These results suggest the tilt axis lies in the plane of the film when ATN is under tensile strain.

Similar to the XRD results, electron diffraction patterns (Figure 2(c)) obtained at room temperature reveal no distinct $1/2\{ooo\} \pm 1/4\{00L\}$ spots. Streaks of diffuse intensity were discernable, suggesting disorder amongst the B-site cations, similar to what was observed in other ATN films and room temperature bulk ATN50/50.[20,24,28]

Complex tilt in ATN on $KTaO_3$

Figure 3 shows synchrotron X-ray diffraction scans through the ATN $1/2(311)$ reflection. In Figure 3(a), no clear peaks are apparent at the quarter-order positions in the H or L directions. However, weak peaks were observed at the $1/2(311) + (01/40)$ position (Figure 3(b)), suggesting that the films do exhibit the complex tilt system, $a^-b^-c^-/a^-b^-c^+$, along an in-plane direction. These results suggest that ATN films under tensile strain are in an M phase at room temperature. Unlike films under compressive strain where the c-axis is oriented along the out-of-plane axis,[20] films under tensile strain have these domains oriented in-plane.

$1/4\{00L\}$ reflections due to local cation displacements

As determined by Levin *et al.*, the three M phases in ATN differ by the degree of ordering of cation displacements.[23] In the highest temperature M3 phase, the displacements of B-site cations are disordered over long-range (short-range ordering along the octahedral chains is manifested in the diffuse scattering seen in Figure 2(c)). Partial ordering of these displacements occurs at the isosymmetric M3 ↔ M2 transition yielding quarter-order reflections about the main Bragg reflections.[23] The ATN films under tensile strain showed no indication of such quarter-order reflections in X-ray or electron diffraction experiments; similar behavior was observed in compressively strained films.[20] This result suggests that either the tensile strain or the point defects in the film disrupt the long-range ordering of the local cation displacements.[28]

TEMPERATURE DEPENDENT RESULTS

The transition temperatures of ATN films under tensile strain were determined by examining the integrated intensities of two superlattice reflections for the ATN on BST/LAO sample. No tilting of the oxygen octahedra exists in the cubic phase and therefore, no associated reflections are expected. In the tetragonal phase, the in-phase tilt will produce $1/2\{ooe\}$-type reflections (where o = odd and e = even).[33] Anti-phase tilting about the a- and b-axes exists in the M phases, producing superlattice reflections of the type $1/2\{ooo\}$. The O phase exhibits a mixed tilt system, $a^0b^-c^+$, which gives rise to anti-phase tilting about the b-axis and in-phase tilting about the

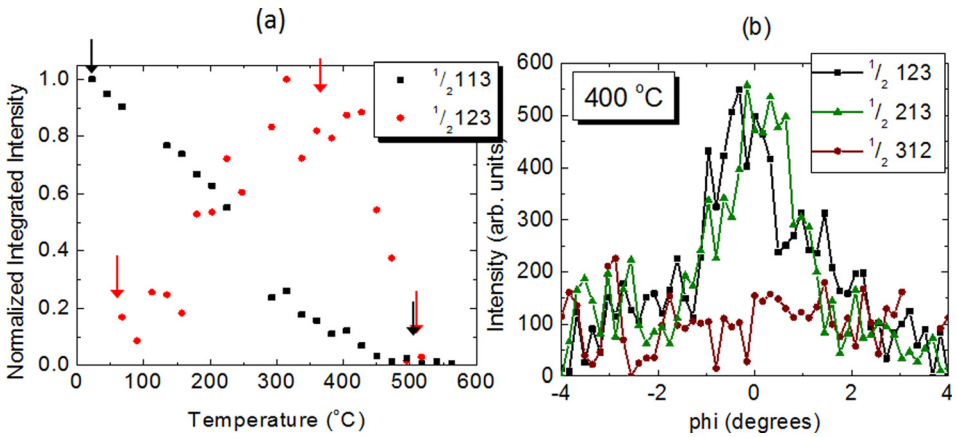

FIG. 4. (a) Normalized integrated intensities of the $1/2(113)$ and $1/2(123)$ reflections as a function of temperature in $Ag(Ta_{0.5}Nb_{0.5})O_3$ films on $(Ba_{0.4}Sr_{0.6})TiO_3/LaAlO_3$. In the M phase, anti-phase tilting dominates; the O phase shows both in-phase and anti-phase tilt and the T phase shows exclusively in-phase tilt. The arrows indicate temperature ranges over which a linear fit was applied to the data in order to determine the phase transition temperature. (b) In-plane rotation phi scans near the $1/2(123)$, $1/2(213)$, and $1/2(312)$ regions in the $Ag(Ta_{0.5}Nb_{0.5})O_3$ /$(Ba_{0.4}Sr_{0.6})TiO_3/LaAlO_3$ sample at 400 °C. The finite intensity of $1/2(123)$ and $1/2(213)$ reflections suggests that the in-phase tilt occurs exclusively around the in-plane axes.

TABLE I. Phase transition temperatures found in bulk $Ag(Ta_{0.5}Nb_{0.5})O_3$ and those determined for $Ag(Ta_{0.5}Nb_{0.5})O_3$ films on a $(Ba_{0.4}Sr_{0.6})TiO_3/LaAlO_3$.

Transition type	Bulk transition temperatures (°C)	Films under tensile strain (°C)
C–T	552	530 ± 95
T–O	400	367 ± 65
O–M_3	326	29 ± 29

c-axis. Figure 4(a) shows the normalized integrated intensity for the ½(113) (anti-phase) and ½(123) peaks (in-phase). When the film is in the M phase, the ½(113) peaks dominate, and when ATN is in the T phase, the ½(123) reflection dominates. Finitie intensity is observed for both superlattice reflections occurs when the material is in the O phase. Interestingly, the intensity of the ½(123) reflection was significantly weaker than a similar reflection in the compressively strained films. This suggests that either the tilt angle or degree of long-range ordering of tilts in ATN under tensile strain is smaller than that in ATN under compressive strain. As a consequence of the weaker intensity of the superlattice reflections, the data shown in Figure 4 are noisier than analogous data for the films on $SrTiO_3$.

The phase transition temperatures were determined by performing linear fits to the integrated intensity data in Figure 4. Arrows in the figure depict the temperature ranges over which the linear fit was applied for both the ½(123) and ½(113) peaks. Table I shows the transition temperatures determined in this work compared to those found in bulk $Ag(Ta_{0.5}Nb_{0.5})O_3$. The error bars were obtained by first fitting a line to the data over the determined temperature range. Error bars for the linear fit were attained from the 95% confidence interval of the fit. After the transition temperature was determined, error propagation was used to calculate the error in the transition temperatures. The results indicate that tensile strain suppresses the M_3-O transition by ~275 °C, while the C-T transition temperature was comparable to bulk. As was observed in compressively strained films, tensile biaxial strain also stabilizes the O and T phase regimes.[20]

The domain state of $Ag(Ta_{0.5}Nb_{0.5})O_3$ thin films on $(Ba_{0.4}Sr_{0.6})TiO_3/LaAlO_3$ was determined through examination of the ½{*ooe*}-type reflections at 400 °C. At this temperature, the material is in the tetragonal phase with the tilt system $a^0a^0c^+$. According to the rules developed by Glazer, the orientation of the tilt axis can be determined.[34] Figure 4(b) shows X-ray diffraction scans of the ½(123), ½(213), and ½(312) reflections. As shown in the figure, non-zero intensity was observed for only the ½(123) and ½(213) peaks, indicating that the in-phase tilt occurs along the in-plane axes. The out-of-plane axis does not show octahedral rotations, as is evidenced by absence of the ½(312) peak. This is in contrast to observations on compressively strained ATN films, where the preferred rotation axis was along the out-of-plane direction.[20] It is, however, in agreement with other reports, which showed that biaxial tensile strain leads to enhancement and suppression of octahedral rotations along the in-plane and out-of-plane axes, respectively.[8,9,35] It can be concluded that in the T phase of tensile-strained ATN films, the tilt axis is along

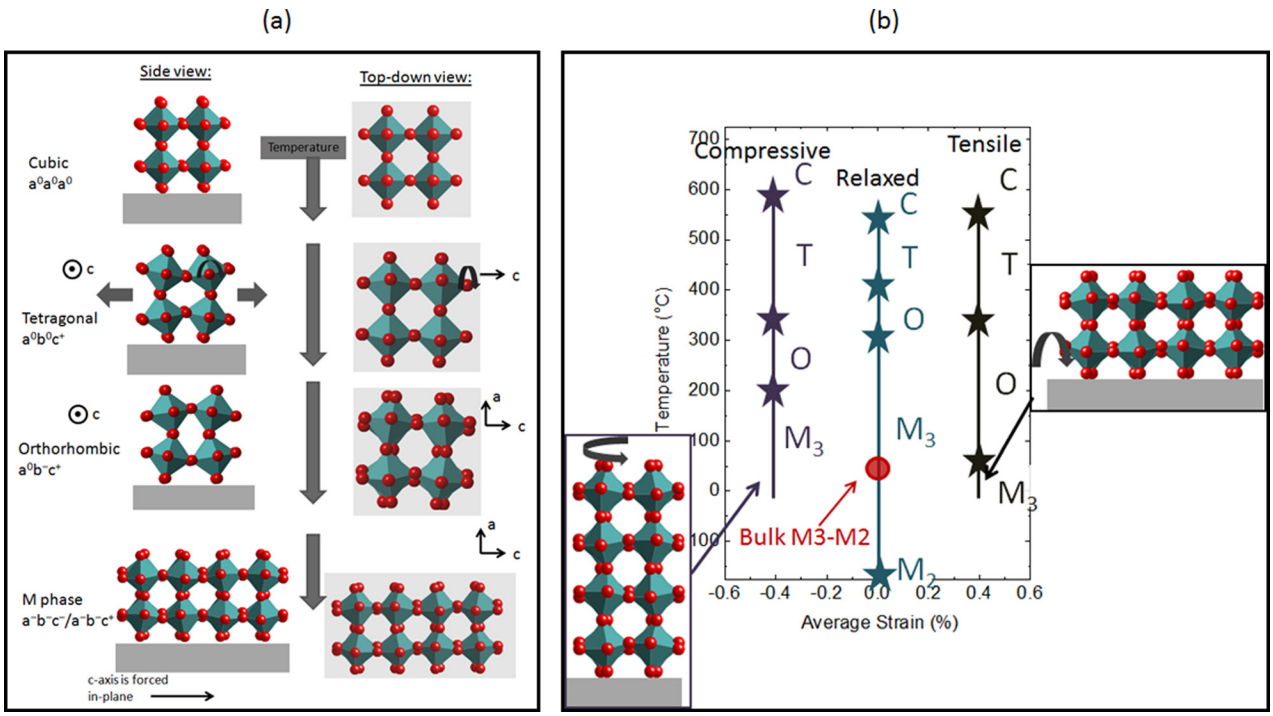

FIG. 5. Schematic illustrating how the domains in ATN under tensile strain (i.e., on a KTO substrate) behave as a function of temperature. At high temperatures, the material is cubic. Then, as it cools through the tetragonal phase, an in-phase tilt develops along the in-plane axes. An anti-phase tilt is added in the O phase. The films are in the M_3 phase at room temperature. The domain structure is such that the complex tilt axis (i.e., the *c*-axis) lies in-plane. In (b), the phase transition temperatures of $Ag(Ta_{0.5}Nb_{0.5})O_3$ films under tensile and compressive stress are summarized on the strain phase diagram and compared to relaxed ATN films of the same composition. The stars indicate phase transitions observed in the respective thin films. The red dot shows the M3-M2 phase transition observed in bulk ATN.

the *c*-axis, suggesting that the domain structure is arranged so that the *c*-axis lies in the film plane.

Figure 5(a) shows a schematic summarizing the evolution of the domain state in ATN films under tensile strain as a function of temperature. When the films are at high temperatures, they are in the cubic phase. As the material cools, it transforms to the T phase with in-phase octahedral tilting about the in-plane axes. It is believed that the tensile strain forces this tilt axis along the in-plane directions to accommodate the smaller out-of-plane lattice parameter required.[10] In the O phase, the ATN film exhibits both anti-phase and in-phase tilts. At room temperature, the films are likely in the M_3 phase, as evidenced by the disappearance of the $^1/_2(123)$ peak. Based on the weak signal of the quarter-order reflections in ATN on $KTaO_3$, it is believed that the *c*-axis resides in the film's plane. As was observed for ATN under compressive strain, it is likely that the activation energy required to reconfigure the octahedral rotations is too high, so that the domain state established at high temperatures templates the room temperature domain structure.

Figure 5(b) shows a compilation of the phase transition temperatures of ATN films under compressive strain, tensile strain, and in a relaxed state. This figure demonstrates that films under compressive or tensile strain show an expanded temperature regime in the O and T phases as compared to relaxed films and bulk ceramics. In addition, there is no indication of the M_2 phase at room temperature for films under either strain state. ATN films under compressive strain were shown to have a domain state in which the complex tilt axis was along the out-of-plane direction.[20] Conversely, as is shown here, the domain structure of ATN films under tensile strain was oriented such that the complex tilt axis was along the in-plane direction. These results are analogous to previous works examining octahedral rotations in simple tilt systems such as $LaNiO_3$ or $LaAlO_3$.[8,9]

CONCLUSIONS

$Ag(Ta_{0.5}Nb_{0.5})O_3$ thin films were deposited on $(Ba_{0.4}Sr_{0.6})TiO_3/LaAlO_3$ $(001)_p$ and $KTaO_3$ (001) substrates. The films were coherent with the substrate and, therefore, subjected to a biaxial tensile stress. Both films were in the M_3 phase at room temperature. It was found that the strain induced in the films created a domain structure with the *c*-axis aligned primarily parallel to the film surface. Both samples exhibited weak intensity of the superlattice reflections, suggesting that either the tilt angle is significantly reduced or the long range order of the complex tilt is suppressed compared to bulk and compressively strained thin films. In addition, the $Ag(Ta_{0.5}Nb_{0.5})O_3$ on $(Ba_{0.4}Sr_{0.6})TiO_3/LaAlO_3$ samples showed an expanded range of temperature stability for the tetragonal and orthorhombic phase fields. This work demonstrates that, in addition to compressive strain, tensile strain can be used to control the domain state and phase transitions of materials with complex tilt systems and phase transition sequences.

ACKNOWLEDGMENTS

Financial support for this work was provided by the National Science Foundation (DMR-0602770, DMR-0820404, and DMR-0908718). Work at Argonne National Laboratory was supported by the U.S. Department of Energy (DOE), Office of Science, Basic Energy Sciences (BES), Materials Sciences and Engineering Division. Use of the Advanced Photon Source was supported by DOE-BES, under Contract No. DE-AC02-06CH11357. The authors would also like to thank Jenia Karapetrova and Pete Baldo for their help at beamline 33-BM at the Advanced Photon Source.

[1]A. Borisevich, O. S. Ovchinnikov, H. J. Chang, M. P. Oxley, P. Yu, J. Seidel, E. A. Eliseev, A. N. Morozovska, R. Ramesh, S. J. Pennycook, and S. V. Kalinin, "Mapping octahedral tilts and polarization across a domain wall in $BiFeO_3$ from Z-contrast scanning transmission electron microscopy image atomic column shape analysis," ACS Nano **4**(10), 6071–6079 (2010).
[2]N. A. Benedek, A. T. Mulder, and C. J. Fennie, "Polar octahedral rotations: A path to new multifunctional materials," J. Solid State Chem. **195**, 11–20 (2012).
[3]J. He, A. Borisevich, S. V. Kalinin, S. J. Pennycook, and S. T. Pantelides, "Control of octahedral tilts and magnetic properties of perovskite oxide heterostructures by substrate symmetry," Phys. Rev. Lett. **105**(22), 227203 (2010).
[4]A. Y. Borisevich, H. J. Chang, M. Huijben, M. P. Oxley, S. Okamoto, M. K. Niranjan, J. D. Burton, E. Y. Tsymbal, Y. H. Chu, P. Yu, R. Ramesh, S. V. Kalinin, and S. J. Pennycook, "Suppression of octahedral tilts and associated changes in electronic properties at epitaxial oxide heterostructure interfaces," Phys. Rev. Lett. **105**(8), 087204 (2010).
[5]Y. M. Kim, A. Kumar, A. Hatt, A. N. Morozovska, A. Tselev, M. D. Biegalski, I. Ivanov, E. A. Eliseev, S. J. Pennycook, J. M. Rondinelli, S. V. Kalinin, and A. Y. Borisevich, "Interplay of octahedral tilts and polar order in $BiFeO_3$ films," Adv. Mater. **25**(17), 2497–2504 (2013).
[6]M. W. Lufaso and P. M. Woodward, "Jahn-Teller distortions, cation ordering and octahedral tilting in perovskites," Acta Crystallogr., Sect. B: Struct. Sci. **60**, 10–20 (2004).
[7]J. M. Rondinelli, S. J. May, and J. W. Freeland, "Control of octahedral connectivity in perovskite oxide heterostructures: An emerging route to multifunctional materials discovery," MRS Bull. **37**(3), 261–270 (2012).
[8]S. J. May, J. W. Kim, J. M. Rondinelli, E. Karapetrova, N. A. Spaldin, A. Bhattacharya, and P. J. Ryan, "Quantifying octahedral rotations in strained perovskite oxide films," Phys. Rev. B **82**(1), 014110 (2010).
[9]R. Johnson-Wilke, D. M. Marincel, S. Zhu, M. P. Warusawithana, A. J. Hatt, J. Sayre, K. T. Delaney, R. Engel-Herbert, C. M. Schleputz, J.-W. Kim, V. Gopalan, N. A. Spaldin, D. G. Schlom, P. J. Ryan, and S. Trolier-McKinstry, "Quantification of octahedral rotations in strained $LaAlO_3$ films via synchrotron X-ray diffraction," Phys. Rev. B **88**, 174101 (2013).
[10]A. J. Hatt and N. A. Spaldin, "Structural phases of strained $LaAlO_3$ driven by octahedral tilt instabilities," Phys. Rev. B **82**(19), 195402 (2010).
[11]E. Bousquet, M. Dawber, N. Stucki, C. Lichtensteiger, P. Hermet, S. Gariglio, J. M. Triscone, and P. Ghosez, "Improper ferroelectricity in perovskite oxide artificial superlattices," Nature **452**(7188), 732–U4 (2008).
[12]S. J. May, C. R. Smith, J.-W. Kim, E. Karapetrova, A. Bhattacharya, and P. J. Ryan, "Control of octahedral rotations in $(LaNiO_3)_n/(SrMnO_3)_m$ superlattices," Phys. Rev. B **83**(15), 153411 (2011).
[13]J. H. Haeni, P. Irvin, W. Chang, R. Uecker, P. Reiche, Y. L. Li, S. Choudhury, W. Tian, M. E. Hawley, B. Craigo, A. K. Tagantsev, X. Q. Pan, S. K. Streiffer, L. Q. Chen, S. W. Kirchoefer, J. Levy, and D. G. Schlom, "Room-temperature ferroelectricity in strained $SrTiO_3$," Nature **430**(7001), 758–761 (2004).
[14]Y. J. Gu, K. Rabe, E. Bousquet, V. Gopalan, and L. Q. Chen, "Phenomenological thermodynamic potential for $CaTiO_3$ single crystals," Phys. Rev. B **85**(6), 064117 (2012).
[15]E. Vlahos, *Phase Transitions and Domain Structures in Multiferroics* (Department of Materials Science and Engineering, The Pennsylvania State University, 2011).
[16]I. M. Reaney, E. L. Colla, and N. Setter, "Dielectric and structural characteristics of Ba-based and Sr-based complex perovskites as a function of tolerance factor," Jpn. J. Appl. Phys., Part 1 **33**(7A), 3984–3990 (1994).
[17]P. M. Woodward, "Octahedral tilting in perovskites 2. Structure stabilizing forces," Acta Crystallogr., Sect. B: Struct. Sci. **53**, 44–66 (1997).
[18]T. T. Fister, H. Zhou, Z. Luo, S. S. A. Seo, S. O. Hruszkewycz, D. L. Proffit, J. A. Eastman, P. H. Fuoss, P. M. Baldo, H. N. Lee, and D. D.

Fong, "Octahedral rotations in strained $LaAlO_3/SrTiO_3$ (001) heterostructures," APL Mater. **2**(2), 021102 (2014).
[19]F. Z. He, B. O. Wells, and S. M. Shapiro, "Strain phase diagram and domain orientation in $SrTiO_3$ thin films," Phys. Rev. Lett. **94**(17), 176101 (2005).
[20]R. L. Johnson-Wilke, D. S. Tinberg, C. B. Yeager, Y. Han, I. M. Reaney, I. Levin, D. D. Fong, T. T. Fister, and S. Trolier-McKinstry, "Tilt transitions in compressively strained $AgTa_{0.5}Nb_{0.5}O_3$ thin films," Phys. Rev. B **84**(13), 134114 (2011).
[21]E. J. Moon, P. V. Balachandran, B. J. Kirby, D. J. Keavney, R. J. Sichel-Tissot, C. M. Schleputz, E. Karapetrova, X. M. Cheng, J. M. Rondinelli, and S. J. May, "Effect of interfacial octahedral behavior in ultrathin manganite films," Nano Lett. **14**(5), 2509–2514 (2014).
[22]C. L. Jia, S. B. Mi, M. Faley, U. Poppe, J. Schubert, and K. Urban, "Oxygen octahedron reconstruction in the $SrTiO_3/LaAlO_3$ heterointerfaces investigated using aberration-corrected ultrahigh-resolution transmission electron microscopy," Phys. Rev. B **79**(8), 081405(R) (2009).
[23]I. Levin, V. Krayzman, J. C. Woicik, J. Karapetrova, T. Proffen, M. G. Tucker, and I. M. Reaney, "Structural changes underlying the diffuse dielectric response in $AgNbO_3$," Phys. Rev. B **79**(10), 104113 (2009).
[24]I. Levin, J. C. Woicik, A. Llobet, M. G. Tucker, V. Krayzman, J. Pokorny, and I. M. Reaney, "Displacive ordering transitions in perovskite-like $AgNb_{1/2}Ta_{1/2}O3$," Chem. Mater. **22**(17), 4987–4995 (2010).
[25]M. Pawelczyk, "Phase-transitions in $AgTa_xNb_{1-x}O_3$ solid-solutions," Phase Transitions **8**(4), 273–292 (1987).
[26]P. Sciau, A. Kania, B. Dkhil, E. Suard, and A. Ratuszna, "Structural investigation of $AgNbO_3$ phases using x-ray and neutron diffraction," J. Phys.: Condens. Matter **16**(16), 2795–2810 (2004).
[27]A. Ratuszna, J. Pawluk, and A. Kania, "Temperature evolution of the crystal structure of $AgNbO_3$," Phase Transitions **76**(6), 611–620 (2003).
[28]Y. Han, I. M. Reaney, R. L. Johnson-Wilke, M. B. Telli, D. S. Tinberg, I. Levin, D. D. Fong, T. T. Fister, S. K. Streiffer, and S. Trolier-McKinstry, "Structural phase transitions in $AgTa_{0.5}Nb_{0.5}O_3$ thin films," J. Appl. Phys. **107**(12), 123517 (2010).
[29]R. L. Johnson-Wilke, D. S. Tinberg, C. Yeager, W. G. Qu, D. D. Fong, T. T. Fister, S. K. Streiffer, Y. S. Han, I. M. Reaney, and S. Trolier-McKinstry, "Coherently strained epitaxial $Pb(Zr_{1-x}Ti_x)O_3$ thin films," J. Appl. Phys. **114**(16), 164104 (2013).
[30]M. B. Telli, S. S. N. Bharadwaja, M. D. Biegalski, and S. Trolier-McKinstry, "(00l) epitaxial $AgTaO_3$ and $AgNbO_3$ thin films on $(001)SrRuO_3/(001)LaAlO_3$ substrates by chemical solution deposition," Appl. Phys. Lett. **89**(25), 252907 (2006).
[31]M. B. Telli, S. S. N. Bharadwaja, M. D. Biegalski, J. G. Cheng, and S. Trolier-McKinstry, "(001) epitaxial $Ag(Ta_{0.5}Nb_{0.5})O_3$ thin films on $(001)SrRuO_3/(001)LaAlO_3$ substrates by chemical solution deposition," J. Appl. Phys. **101**(1), 014111 (2007).
[32]M. B. Telli, "Chemical solution deposition of silver tantalate niobate, $Ag(Ta_xNb_{1-x})O_3$, thin films," PhD dissertation (Materials Science and Engineering, The Pennsylvania State University, University Park, PA, USA, 2005).
[33]D. I. Woodward and I. M. Reaney, "Electron diffraction of tilted perovskites," Acta Crystallogr. Sect. B: Struct. Sci. **61**, 387–399 (2005).
[34]A. M. Glazer, "Simple ways of determining perovskite structures," Acta Crystallogr., Sect. A **31**, 756–762 (1975).
[35]A. Vailionis, H. Boschker, W. Siemons, E. P. Houwman, D. H. A. Blank, G. Rijnders, and G. Koster, "Misfit strain accommodation in epitaxial ABO_3 perovskites: Lattice rotations and lattice modulations," Phys. Rev. B **83**(6), 064101 (2011).